

**Title**

Effects of ATP and analogues on  $[Ca^{2+}]_i$  dynamics in the rabbit corneal epithelium

**Authors**

Katsura KIMURA<sup>1,2</sup>, Tomoko NISHIMURA<sup>1,2</sup>, and Yoh-ichi SATOH<sup>1</sup>

From the Departments of Histology<sup>1</sup> and Ophthalmology<sup>2</sup>, Iwate Medical University School of Medicine, Morioka, Japan.

**Grant support**

This work was supported by research grants from the Ministry of Education, Culture and Science of Japan (Y.S.; 08457007) and from the Promotion and Mutual Aid Corporation for Private Schools of Japan.

**Correspondence**

Dr. Y. SATOH

Department of Anatomy 2 (Histology), Iwate Medical University School of Medicine  
19-1 Uchimaru, Morioka, Iwate, 020-8505 Japan.

佐藤洋一

020-8505

岩手県盛岡市内丸 19-1

岩手医科大学医学部解剖学第2講座

Tel: +81-19-651-5111

Fax: +81-19-651-5605

E-mail: yisatoh@iwate-med.ac.jp

佐藤洋一



**Summary.** Adenosine-5'-triphosphate (ATP) plays a pivotal role in various tissues as an extracellular transmitter. ATP released from nerve endings and/or damaged cells may elicit reactions in adjacent cells. To identify such reactions, we investigated the dynamics of the intracellular calcium ion concentration ( $[Ca^{2+}]_i$ ) in the rabbit corneal epithelium during ATP-stimulation. Intact epithelial sheets isolated from corneal tissue were loaded with Fura-2, and  $[Ca^{2+}]_i$  dynamics in each cell layer were analyzed using a digital imaging system (Argus50/CA). Normal architecture was preserved, suggesting that functional integrity remained intact. Perfusion with HEPES-buffered Ringer's solution (HR) containing ATP (10  $\mu$ M) and uridine-5'-triphosphate (UTP; 10  $\mu$ M) caused a biphasic  $[Ca^{2+}]_i$  increase in the superficial layer that manifested as a rapid initial spike followed by a long-lasting plateau phase. Adenosine-5'-diphosphate (ADP; 10  $\mu$ M) elevated the  $[Ca^{2+}]_i$  level, but induced only the initial spike, which was smaller than those induced by ATP and UTP. Adenosine (10  $\mu$ M) did not elicit any  $[Ca^{2+}]_i$  changes in the epithelial cells. Suramin (10  $\mu$ M; a P2 receptor antagonist) blocked the ATP-induced  $[Ca^{2+}]_i$  increase, whereas the P2X receptor agonists,  $\alpha,\beta$ -methylene ATP (10  $\mu$ M), 2-methylthio ATP (10  $\mu$ M) and Benzoylbenzoyl ATP (10  $\mu$ M), did not elicit any increases in  $[Ca^{2+}]_i$ . In the basal cell layer, ATP-induced  $[Ca^{2+}]_i$  dynamics were biphasic, while oscillatory fluctuations of  $[Ca^{2+}]_i$  were induced in the wing cells of the mid layer of the corneal epithelium by ATP stimulation.  $Ca^{2+}$  oscillations were sometimes synchronized among adjacent wing cells but these waves did not propagate to other layers of cells. These results suggest that extracellular ATP elicits a  $[Ca^{2+}]_i$  increase mainly via P2Y receptors. More interestingly, synchronized  $Ca^{2+}$  oscillation in the wing cell layer indicates that intracellular events may spread to neighboring cells within the layer.

Adenosine triphosphate (ATP) is a principal high-energy intermediate compound found in living cells. In addition, ATP is present in extracellular spaces, since nerve endings in most peripheral nervous systems secrete it together with neurotransmitters and ATP leaks from injured cells (BURNSTOCK, 1996; NEARY et al., 1996). Increasing evidence indicates that extracellular adenosine (a breakdown product of ATP) and ATP acts as an extracellular signal that controls cell function via receptors in the cell membrane. Receptors for adenosine and ATP are classified into P1 (or designated as A1-3) and P2 types, respectively (DUBYAK, 1991; NEARY et al., 1996; FREDHOLM et al., 1997). According to pharmacological criteria, P2-receptors are grouped into several families (P2X<sub>1-7</sub> and P2Y<sub>1-11</sub>) (KUNAPULI and DANIEL, 1998).

Intracellular calcium ion concentration ( $[Ca^{2+}]_i$ ) dynamics constitute a ubiquitous intracellular signaling system (BERRIDGE et al., 1998), and extracellular ATP induces  $[Ca^{2+}]_i$  dynamics in various tissues, including ocular tissues such as corneal endothelial cells (CRAWFORD et al., 1993; SRINIVAS et al., 1998), lens epithelial cells (RIACH et al., 1995; DUNCAN et al., 1996; CHURCHILL and LOUIS, 1997), ciliary epithelial cells (SUZUKI et al., 1997) and the retina (KIRISCHUK et al., 1995; SAKAKI et al., 1996; SUGIOKA et al., 1996; LIU and WAKAKURA, 1998). The  $[Ca^{2+}]_i$  is changed in isolated/cultured cells of the corneal epithelium by methoxamine (an  $\alpha_1$ -agonist), carbachol (a muscarinic agonist) and endothelins (peptides derived from endothelium during vasoconstriction) (REINACH et al., 1992; TAKAGI et al., 1994; SOCCI et al., 1996; TAO et al., 1997). ATP is released from physically stimulated cells (ENOMOTO et al., 1994) and/or nerve endings (BURNSTOCK, 1996) have been reported in various tissues and cells, therefore in addition to the agonists described above, extracellular ATP may affect the  $[Ca^{2+}]_i$  dynamics of corneal epithelial cells, as a result of vulnerability to external wounds and the rich nerve supply to the corneal epithelium

(MACIVER and TANELIAN, 1993). However, the effect of ATP on corneal epithelial cells has not yet been investigated.

$[Ca^{2+}]_i$  dynamics have often been measured, but mostly in isolated/cultured cells were obtained from various tissues including neoplasm. However, such isolated/cultured cells are in many cases difficult to maintain the structural and functional characteristics of the cells in tissues. When these cells are used for the measurement of  $[Ca^{2+}]_i$  dynamics, physiologically important reactions may be modified by various artifacts. Intercellular communication accompanied by a  $[Ca^{2+}]_i$  increase has been identified in cultured cells in vitro (SANDERSON, 1996), but it whether or not this process occurs in normal tissues has not been studied.

Stratified corneal epithelium is composed of a superficial cell layer, a wing cell layer in the mid region and a basal cell layer located on the stroma. Therefore, in the present study, we decide to prepare epithelial sheets of cornea to determine  $[Ca^{2+}]_i$  dynamics elicited by ATP. This model is convenient for studying not only local changes in  $[Ca^{2+}]_i$  occurring within a single cell or in small masses of epithelial cells possessing essential structural integrity, but also intercellular communications in the tissue.

The present study initially examined whether or not extracellular ATP and its analogues elicit  $[Ca^{2+}]_i$  response of within epithelial sheets prepared from the rabbit cornea.  $[Ca^{2+}]_i$  dynamics were analyzed by digital imaging using a fluorescent microscope. We also examined regional differences of ATP-induced  $[Ca^{2+}]_i$  dynamics and discuss the possibility of intercellular communications in the corneal epithelium.

## MATERIALS AND METHODS

### Preparation of corneal epithelium

Japan white rabbits (adult, male, weighing 2.0-2.5 kg) were euthanized by an overdose (2 mg/kg in body weight) of pentobarbital (Abbott, North Chicago, IL, USA) injected into a marginal ear vein. After removing eye globes, the cornea were cut along the limbus. The endothelium and Descemet's membrane were removed under a binocular microscope and the remaining epithelium and stroma were cut into several pieces in HEPES-buffered Ringer's solution (HR). Tissue pieces were placed in HR containing dispase (2.0 units/ml; Worthington, Freehold, NJ, USA) and shaken for 60 min at 37 °C. Epithelial sheets were then gently dissected free of stroma and disrupted by pipetting in HR before centrifugation at 2,000 rpm for 5 min twice. The sediment was resuspended in enzyme-free HR. Experiments were performed within 12 h after tissue isolation. Standard HR (pH 7.4, adjusted with NaOH) contained 118 mM NaCl, 4.7 mM KCl, 1.25 mM CaCl<sub>2</sub>, 1.13 mM MgCl<sub>2</sub>, 1.0 mM Na<sub>2</sub>HPO<sub>4</sub>, 10 mM D-glucose, 2.0 mM sodium glutamate, 10 mM HEPES, MEM amino acid solution (Gibco, Grand Island, NY, USA) and 0.2% bovine serum albumin (Sigma, St. Louis, MO, USA).

### Loading of Ca<sup>2+</sup>-sensitive dyes and stimulation

We analyzed spatiotemporal changes in [Ca<sup>2+</sup>]<sub>i</sub> levels by ratiometry of the fluorescent dye, Fura-2. The spectral shift of Fura-2 binding to Ca<sup>2+</sup> indicates the Ca<sup>2+</sup> concentration (GRYNKIEWICZ et al., 1985). Acetoxymethyl esters of the dye (Fura-2/AM; Dojindo, Kumamoto, Japan) facilitated loading.

Epithelial specimens were placed so that the basal surface faced up or down on coverslips coated with Cell-Tak (Collaborative Biomedical, Bedford, MA, USA) in modified

Sykus-Moor chambers. Some specimens were attached with the superficial layer facing the coverslips. Fura-2/AM (1  $\mu$ M) was loaded at room temperature (20-25 °C) for 45 min.

The specimens were continuously perfused with HR containing the following agonists and/or antagonists: adenosine 5'-triphosphate (ATP; Kohjin, Tokyo, Japan), adenosine 5'-diphosphate (ADP; Sigma), adenosine 5'-monophosphate (AMP; Sigma), uridine 5'-diphosphate (UTP; Sigma),  $\alpha,\beta$ -methylene ATP ( $\alpha,\beta$ -meATP; Sigma), benzoylbenzoyl ATP (BzATP; Sigma), adenosine (Sigma), 2-methylthio ATP (2-MeSATP; Research Biochemicals International, Natick, MA, USA), thapsigargin (Alomone Lab, Jerusalem, Israel) and/or suramin (Research Biochemicals International).

#### Acquisition of digital images showing $[Ca^{2+}]_i$ dynamics

Fura-2 fluorescence (510 nm) emitted during excitation at 380 nm and 340 nm was digitally imaged using an inverted microscope (IX70 with an UApo 40/340, N.A.0.90 objective; Olympus, Tokyo, Japan), a digital image processor (Argus 50/CA; Hamamatsu Photonics, Hamamatsu, Japan), and an intensified Charged-coupled device camera (C240087; Hamamatsu Photonics). Successive pairs of digital images were obtained at 5 sec intervals. Thereafter, the ratio of the fluorescent intensity of cells excited at 340 nm and 380 nm (F340/F380) was converted to  $[Ca^{2+}]_i$  using the Argus 50/CA. Peripherally located cells of epithelial specimens were loaded with more Fura-2 than centrally located cells. However, artifacts caused by variations in the dye concentration were minimized using ratiometry. Digital images showing  $[Ca^{2+}]_i$  were displayed using 4 bit pseudocolor (spatial analysis). In the color table of the ratio image, red represents high  $[Ca^{2+}]_i$  and blue represent low  $[Ca^{2+}]_i$ . Several areas of  $[Ca^{2+}]_i$  dynamics representing about 4  $\mu$ m<sup>2</sup> located in the periphery or center of the specimen image were selected, and consecutive  $[Ca^{2+}]_i$  changes at various points were

analyzed (temporal analysis).

The F340/F380 values of a series of Fura-2 solutions with  $\text{Ca}^{2+}$  concentrations ranging from 0 to 1,350 nM (Calcium calibration buffer kit #2; Molecular Probes, Eugene, OR, USA) were measured to obtain calibration curves. However, the dissociation constant of Fura-2 for  $\text{Ca}^{2+}$  in the cytoplasm differs from that measured in the absence of proteins. Therefore,  $[\text{Ca}^{2+}]_i$  values obtained from calibration curves may not represent actual values.

#### *Ultrastructure and viability of specimens*

We elucidated the morphological integrity of specimens of the corneal epithelium by electron microscopy. After measuring  $[\text{Ca}^{2+}]_i$  dynamics, epithelial specimens were fixed in 0.25% glutaraldehyde and 4% paraformaldehyde in phosphate-buffered saline (PBS; 0.1 M) for about 4 h. The specimens were then postfixed in 1% osmium tetroxide in PBS for 1 h at 4°C, dehydrated in a graded ethanol series and embedded in Epon 812 (TAAB, Berkshire, England). We cut consecutively vertical sections through the cornea using an ultramicrotome (2088 ULTROTOME; LKB, Bromma, Sweden). Semithin sections (about 1  $\mu\text{m}$  thick) stained with toluidine blue and ultrathin sections (about 0.07  $\mu\text{m}$  thick) doubly stained with uranyl acetate and lead citrate were examined under light and electron microscopes (H-7100; Hitachi Co, Hitachi, Japan), respectively. Non-treated fresh cornea tissue fixed and processed for electron microscopy as described above was used as a control.

To confirm the viability of epithelial cells, some specimens were incubated in HR containing 1  $\mu\text{M}$  ethidium homodimer-1 (EthD-1; a fluorescent dye that binds to DNA; Molecular Probes) for 5 min at room temperature. Cells with active transport mechanisms that are damaged during isolation procedures can not extrude the dye, and therefore fluoresce orange-red (emitted at 580 nm by the excitation at 520-550 nm), whereas intact cells do not

(POOLE et al., 1993).

## RESULTS

### *Structure and viability of corneal epithelium*

We measured  $[Ca^{2+}]_i$  levels in the corneal epithelium that retained the superficial, wing and basal cell layers (Figs. 1a; 2a). Most specimens were slightly dome-shaped; the superficial layer had a convex profile and the basal cell layer took a concave profile. It is possible to assume that the periphery of fluorescent images of these specimens mainly represented the superficial cell layer when the focal plane was adjusted to the wing cell layer of the epithelial sheet (Fig. 1b).

Electron microscopy revealed normal ultrastructure in the specimens. No structural difference was detected between controls and the epithelial specimens for  $[Ca^{2+}]_i$  measurement. Adjacent cells were articulated by desmosomes and intercellular spaces did not expand, suggesting normal intercellular communication (Fig. 2b). We found a few cisternal profiles of the endoplasmic reticulum (ER), which is considered as an intercellular  $Ca^{2+}$  store (Fig. 2b). These findings indicated that structural integrity was maintained in these specimens. Additionally, few cells of the specimens emitted red fluorescence after the incubation of EthD-1 (Fig. 3a, b). We therefore concluded that the epithelial sheets preserved the normal transport mechanisms of the cell membrane. These mechanisms are for intracellular signaling.

### *ATP-induced $[Ca^{2+}]_i$ dynamics in superficial layer of corneal epithelium*

The amount of fluoresce emitted the superficial layer was sufficiently intense and stable for image acquisition. Therefore, we initially examined ATP-induced  $[Ca^{2+}]_i$  dynamics in the superficial cell layer. Under resting conditions, the  $[Ca^{2+}]_i$  was about  $48.6 \pm 7.5$  nM (number of independent chambers analyzed,  $n = 11$ ), with no apparent fluctuation. Extracellular ATP

(10  $\mu\text{M}$ ) caused a biphasic response with the first phase consisting of a rapid increase in  $[\text{Ca}^{2+}]_i$  (spike phase) and the second phase consisting a sustaining in  $[\text{Ca}^{2+}]_i$  increase (plateau phase). After washing out residual ATP, the  $[\text{Ca}^{2+}]_i$  level rapidly decreased to the baseline ( $n = 11$ ) (Fig. 4).

To determine whether ATP-induced  $[\text{Ca}^{2+}]_i$  increase was due to an influx of extracellular  $\text{Ca}^{2+}$  or a release of  $\text{Ca}^{2+}$  from intracellular stores, specimens were stimulated by ATP in the absence of extracellular  $\text{Ca}^{2+}$ . Removal of extracellular  $\text{Ca}^{2+}$  did not affect the spike phase of ATP-induced  $[\text{Ca}^{2+}]_i$  dynamics, but the plateau phase was abolished ( $n = 6$ ) (Fig. 5a).

$\text{Ca}^{2+}$  leaks spontaneously from intracellular  $\text{Ca}^{2+}$  store, and the excess  $\text{Ca}^{2+}$  is normally transported back into the store. Thapsigargin is an inhibitor of sarco-endoplasmic reticulum  $\text{Ca}^{2+}$ -ATPase, and blocks reuptake of  $\text{Ca}^{2+}$  into sarco-endoplasmic reticulum, which is an intracellular  $\text{Ca}^{2+}$  store (THASTRUP et al., 1990). Consequently, thapsigargin (1  $\mu\text{M}$ ) resulted in a gradual increase of  $[\text{Ca}^{2+}]_i$ . After depleting intracellular  $\text{Ca}^{2+}$  stores using thapsigargin, ATP did not induce further  $[\text{Ca}^{2+}]_i$  dynamics ( $n = 6$ ) (Fig. 5b). The results indicate that the spike phase of ATP-induced  $[\text{Ca}^{2+}]_i$  dynamics is caused by  $\text{Ca}^{2+}$  release from the intracellular  $\text{Ca}^{2+}$  store, and the plateau phase depends on  $\text{Ca}^{2+}$  influx.

#### *Effects ATP-analogues and of antagonists*

Adenosine (10  $\mu\text{M}$ ; a P1 receptor agonist) did not increase  $[\text{Ca}^{2+}]_i$  levels ( $n = 8$ ) (Fig. 6a).

Suramin (100  $\mu\text{M}$ ; a P2 receptor antagonist) (MALLARD et al., 1992) totally inhibited ATP-induced  $[\text{Ca}^{2+}]_i$  dynamics ( $n = 7$ ) (Fig. 6b).

UTP (10  $\mu\text{M}$ ; a P2Y<sub>2,4</sub> receptor agonist) caused a biphasic type of  $[\text{Ca}^{2+}]_i$  increase like that induced by ATP ( $n = 7$ ) (Fig. 7a). ADP (10  $\mu\text{M}$ ) caused only an initial spike phase

(n = 7; Fig. 7b).  $\alpha,\beta$ -meATP (10  $\mu$ M; a P2X<sub>1</sub> receptor agonist), 2-MeSATP (10  $\mu$ M; a P2X<sub>3</sub> receptor agonist) and BzATP (10  $\mu$ M; a P2X<sub>7</sub> receptor agonist) induced no significant change in [Ca<sup>2+</sup>]<sub>i</sub> (n = 9, 8 and 5, respectively) (Fig. 7c, d).

#### *Different responses among layers of corneal epithelium*

The ATP-induced [Ca<sup>2+</sup>]<sub>i</sub> increases in the basal cell layer were biphasic (n = 6) and consisted of spike and plateau phases, similar to those of the superficial layer (Fig. 8a, c). However, responses of the wing cell layer to ATP differed. After the spike in the acute [Ca<sup>2+</sup>]<sub>i</sub> increase, oscillatory fluctuations of [Ca<sup>2+</sup>]<sub>i</sub> (calcium oscillation) appeared at intervals of 20-40 seconds (n = 18) (Fig. 8a, b). The peak level of [Ca<sup>2+</sup>]<sub>i</sub> during these oscillations decayed over time. ATP-induced Ca<sup>2+</sup> oscillations were often synchronized among wing cells (Fig. 8b).

Oscillation in one region persisted during ATP stimulation, but that in others was repeated only a few times (data not shown). Oscillatory fluctuations in the wing cell layer was not propagated to other two layers.

## DISCUSSION

The present study discovered that extracellular ATP caused a significant increase in  $[Ca^{2+}]_i$  in the corneal epithelium, and that oscillatory fluctuations of  $[Ca^{2+}]_i$  dynamics were often synchronized in wing cell layer.

### *ATP-induced $[Ca^{2+}]_i$ dynamics*

ATP may have acted directly on P2 receptors or via P1 receptors after ectoenzymic breakdown to adenosine. In the present study, adenosine did not increase  $[Ca^{2+}]_i$  and suramin blocked ATP-induced  $[Ca^{2+}]_i$  dynamics, indicating that ATP-induced  $[Ca^{2+}]_i$  dynamics were caused via P2 receptors.

P2 receptors belong to the following two major families; P2X, which has ligand-gated cation channels and P2Y, which consists of seven membrane-spanning receptors coupled to G proteins. The activated G proteins stimulate phospholipase C, which hydrolyses phosphatidylinositol 4,5-bisphosphate to inositol 1,4,5-triphosphate which in turn causes  $Ca^{2+}$  release from intracellular stores (BERRIDGE, 1993). Another that opens non-selective pores might belong to the P2X family (P2X<sub>7</sub>; previously described as P2Z). Our results indicated that the spike phase could be caused by the release of  $Ca^{2+}$  from intracellular stores, whereas the plateau phase seemed to be maintained by an influx of extracellular  $Ca^{2+}$ . Therefore, we initially expected that the spike phase of  $[Ca^{2+}]_i$  dynamics may have been caused via P2Y receptors and the plateau phase via P2X receptors. This supposition was examined by stimulation with ATP-analogues.

P2 receptor families have different potential for ATP-analogues, and based on the order of potency, (BURNSTOCK, 1996). In the present study, the rank order of P2 receptor agonists was ATP = UTP  $\gg$  ADP, whereas  $\alpha,\beta$ -meATP, 2-MeSATP and BzATP were inactive. This order of potency indicates that the P2Y receptor plays a role in ATP-induced  $[Ca^{2+}]_i$

dynamics in the corneal epithelium. We found that the potent agonist of P2X receptors,  $\alpha,\beta$ -meATP and BzATP had no effect and that UTP, which does not stimulate P2X receptors, caused the plateau phase. Thus, contrary to our initial notion, the plateau phase was not caused via P2X receptors, but by P2Y receptors. The  $\text{Ca}^{2+}$  influx in the plateau phase might operate through a capacitative ( $\text{Ca}^{2+}$  store dependent) mechanism (FASOLATO et al., 1994). Definitive evidence of capacitative  $\text{Ca}^{2+}$  entry in corneal epithelial cells has proven elusive.

#### *Oscillatory fluctuations in $[\text{Ca}^{2+}]_i$ of corneal epithelial cells*

Since the specimens retained essential structural integrity, we found that ATP-induced  $[\text{Ca}^{2+}]_i$  dynamics differed among the corneal epithelial cell layers. In the superficial and basal cell layers, ATP-induced  $[\text{Ca}^{2+}]_i$  increases were biphasic. On the other hand, ATP caused oscillatory fluctuations in the wing cell layer. We are the first to report that  $[\text{Ca}^{2+}]_i$  dynamics in the corneal epithelium are heterogeneous, and this indicates that the stage of cytodifferentiation has different potential for  $[\text{Ca}^{2+}]_i$  dynamics.

Oscillatory fluctuations in  $[\text{Ca}^{2+}]_i$  dynamics have been observed in various ocular tissues, such as corneal endothelial (CRAWFORD et al., 1993), lens epithelial (RIACH et al., 1995) and ciliary epithelial cells (GINOVANELLI et al., 1996). However, the physiological significance of the calcium oscillation in these tissues had remained obscure. A recent study showed that calcium oscillation regulates specific gene transcription (LI et al., 1998). Calcium oscillation of wing cell layer of cornea may play a role in the differentiation of corneal epithelium.

Repetitive intercellular calcium waves accompanied by calcium oscillations (SANDERSON et al., 1994) may represent a general mechanism of intercellular communication. In the present study, the ATP-induced  $[\text{Ca}^{2+}]_i$  increase in calcium oscillations became synchronized among adjacent cells in the wing cell layer, indicating a intercellular

communication mechanism in the wing cell layer.

Intercellular calcium waves can propagate between cells via gap junctions (SANDERSON et al., 1990, 1994; CHARLES et al., 1992). The rabbit corneal epithelium contains connexin 43 and 50 in both the basal and wing cell layers, and gap junctional intercellular communication can regulate wound-healing in the cornea (MATIC et al., 1997). However,  $[Ca^{2+}]_i$  dynamics of wing cells did not affect on those of basal cells, although the basal cell layer contains also connexin 43. In accordance with the present results, intercellular dye diffusion between different cell layers was highly restricted (WOLOSIN, 1991). Therefore, intercellular communications in the corneal epithelium may be regulated not only by gap junctions but also by other factors at various stages of cytodifferentiation.

In conclusion, extracellular ATP can affect the intracellular signaling linked with  $[Ca^{2+}]_i$  dynamics of the corneal epithelium which posses P2Y receptors and the ATP-induced response is intercellulaly conveyed to adjacent cells. ATP is probably indispensable for maintaining the integrity of the corneal epithelium. Further studies using the confocal microscope with highly spatial resolution will reveal whether the nerve endings in corneal epithelium

**Acknowledgments:** We thank Prof. Yutaka Tazawa, Department of Ophthalmology, for his critical reviewing and encouragement during this study, and also thank Mr. K. Kumagai and Mr. H. Satou, Department of Histology, for skillful technical assistance.

## REFERENCES

- BERRIDGE, M. J.: Inositol triphosphate and calcium signaling. *Nature* 361, 315-325 (1993).
- BERRIDGE, M. J., M. D. BOOTMAN and P. LIPP: Calcium -a life and death signal. *Nature*. 395: 645-648 (1998).
- BURNSTOCK, G.: P2 purinoceptors: historical perspective and classification. In: CHADWICK, D.J and GOODE, J.A eds. P2 purinoceptors: localization, function and transduction mechanisms: Chiba Foundation Symposium 198. New York: JOHN WILEY & SONS 1996 (p1-34).
- CHARLES, A.C., C. C. NAUS., D. ZHU., G. M. KIDDER., E. R. DIRKSEN and M. J. SANDERSON: Intercellular calcium signaling via gap junctions in glioma cells. *J. Cell Biol.* 118: 195-201 (1992).
- CHURCHILL, G. C. and C. F. LOUIS: Stimulation of P2U purinergic or alpha 1A adrenergic receptors mobilizes Ca<sup>2+</sup> in lens cells. *Invest. Ophthalmol. Vis. Sci.* 38: 855-865 (1997).
- CRAWFORD, K. M., D. K. MACCALLUM and S.A. ERNST: Agonist-induced Ca<sup>2+</sup> mobilization in cultured bovine and human corneal endothelial cells. *Curr. Eye Res.* 12: 303-311 (1993).
- DUBYAK, G. R.: Signal transduction by P2-purinergic receptors for extracellular ATP. *Am. J. Resp. Cell Mol.* 4: 295-300 (1991).
- DUNCAN, G., R. A. RIACH., M. R. WILLIAMS., S. F. Webb., A. P. DAWSON and J. R. Reddan: Calcium mobilization modulates growth of lens cells. *Cell Calcium.* 19: 83-89 (1996).
- ENOMOTO, K., K. FURUYA, S. YAMAGISHI, T. OKA and T. MAENO: The increase in the intracellular Ca<sup>2+</sup> concentration induced by mechanical stimulation is propagated via

- release of pyrophosphorylated nucleotides in mammary epithelial cells. *Pflügers Arch.* 427: 533-542 (1994).
- FASOLATO, C., B. INNOCENTI and T. POZZAN: Receptor-activated  $Ca^{2+}$  influx: how many mechanisms for how many channels? *Trend. Pharmacol. Sci.* 15: 77-83 (1994).
- FREDHOLM, B. B., M. P. ABBRACCHIO., G. BURNSTOCK., G. R. DUBYAK., T. K. HARDEN., K. A. JACOBSON., U. SCHWABE and M. WILLIAMS: Towards a revised nomenclature for P1 and P2 receptors. *Trend. Pharmacol. Sci.* 18: 79-82 (1997).
- GIOVANELLI, A., S. FUCILE., A. MEAD., E. MATTEI., F. EUSEBI and M. SEARS: Spontaneous and evoked oscillations of cytosolic calcium in the freshly prepared ciliary epithelial bilayer of the rabbit eye. *Biochem. Biophys. Res. Com.* 220: 472-477 (1996).
- GRYNKIEWICZ, G., M. POENIE and R. Y. TSIEN: A new generation of  $Ca^{2+}$  indicators with greatly improved fluorescence properties. *J. Biol Chem.* 260: 3440-3450 (1985).
- KIRISCHUK, S., J. SCHERER., H. KETTENMANN and A. VERKHRATSKY: Activation of P2-purinoreceptors triggered  $Ca^{2+}$  release from InsP3-sensitive internal stores in mammalian oligodendrocytes. *J. Physiol.* 483: 41-57 (1995).
- KUNAPULI, S. P and J. L. DANIEL: P2 receptor subtypes in the cardiovascular. *Biochem. J.* 336: 513-523 (1998).
- LI, W-h., J. LLOPIS., M. WHITNEY., G. ZLOKARNIK and R.Y. TSIEN: Cell-permeant caged InsP3 ester shows that  $Ca^{2+}$  spike frequency can optimize gene expression. *Nature.* 392: 936-941 (1998).
- LIU, Y and M. WAKAKURA: P1-/P2-purinergic receptors on cultured rabbit retinal Müller cells. *Jpn. J. Ophthalmol.* 42: 33-40 (1998).
- MACIVER, M. B and D. L. TANELIAN: Free nerve ending terminal morphology is fiber

- type specific for A delta and C fibers innervating rabbit corneal epithelium. *J. Neurophysiol.* 69: 1779-1783 (1993).
- MALLARD, N., R. MARSHALL., A. SITHERS and B. SPRIGGS: Suramin: a selective inhibitor of purinergic neurotransmission in the rat isolated vas deferens. *Eur. J. Pharmacol.* 220: 1-10 (1992).
- MATIC, M., I. N. PETROU., T. ROSENFELD and J. M. WOLOSIN: Alterations in connexin expression and cell communication in healing corneal epithelium. *Invest.Ophthalmol. Vis. Sci.* 38: 600-609 (1997).
- NEARY, J. T., M. P. RATHBONE., F. CATTABENI., M. P. ABBRACCHIO and G. BURNSTOCK: Trophic actions of extracellular nucleotides and nucleosides on glial and neuronal cells. *Trends. Neurosci.* 19: 13-18 (1996).
- POOLE, C. A., N. H. BROOKES and G. M. CLOVER: Keratocyte networks visualised in the living cornea using vital dyes. *J. Cell Sci.* 106: 685-691 (1993).
- REINACH, P. S., R. R. SOCCI., C. KEITH and M. SCANLON: Adrenergic receptor-mediated increase of intracellular  $Ca^{2+}$  concentration in isolated bovine corneal epithelial cells. *Comp. Biochem. Physiol.* 102: 709-714 (1992).
- RIACH, R. A., G. DUNCAN., M. R. WILLIAMS and S. F. WEBB: Histamine and ATP mobilize calcium by activation of H1 and P2u receptors in human lens epithelial cells. *J. Physiol.* 486: 273-282 (1995).
- SAKAKI, Y., Y. FUKUDA and M. YAMASHITA: Muscarinic and purinergic  $Ca^{2+}$  mobilizations in the neural retina of early embryonic chick. *Int. J. Devel Neurosci.* 14: 691-699 (1996).
- SANDERSON, M. J.: Intercellular waves of communication. *News Physiol. Sci.* 11: 262-269 (1996).

- SANDERSON, M. J., A. C. CHARLES and E. R. DIRKSEN: Mechanical stimulation and intercellular communication increases intracellular  $Ca^{2+}$  in epithelial cells. *Cell. Regul.* 1:585-596 (1990).
- SANDERSON, M. J., A. C. CHARLES., S. BOITANO and E. R. DIRKSEN: Mechanisms and function of intercellular calcium signaling. *Mol. Cellular Endocrinol.* 98:173-187 (1994).
- SOCCI, R. R., S. D. TACHADO., R. S. ARONSTAM and P. S. REINACH: Characterization of the muscarinic receptor subtypes in the bovine corneal epithelial cells. *J. Ocul Pharmacol. Th.* 12: 259-269 (1996).
- SRINIVAS, S. P., J. C. YEH., A. ONG and J. A. BONANNO:  $Ca^{2+}$  mobilization in bovine corneal endothelial cells by P2 purinergic receptors. *Curr. Eye Res.* 17: 994-1004 (1998).
- SUGIOKA, M., Y. FUKUDA and M. YAMASHITA:  $Ca^{2+}$  responses to ATP via purinoceptors in the early embryonic chick retina. *J. Physiol.* 493: 855-863 (1996).
- SUZUKI, Y., T. NAKANO and M. SEARS: Calcium signals from intact rabbit ciliary epithelium observed with confocal microscopy. *Curr. Eye Res.* 16:166-175 (1997).
- TAKAGI, H., P. S. REINACH., S.D. TACHADO and N. YOSHIMURA: Endothelin-mediated cell signaling and proliferation in cultured rabbit corneal epithelial cells. *Invest. Ophthalmol. Vis. Sci.* 35: 134-142 (1994).
- TAO, W., X. WU., G. I. LIOU., T. O. ABNEY and P. S. REINACH: Endothelin receptor-mediated  $Ca^{2+}$  signaling and isoform expression in bovine corneal epithelial cells. *Invest. Ophthalmol. Vis. Sci.* 38: 130-141 (1997).
- THASTRUP, O., P. J. CULLEN., B. K. DROBAK., M. R. HANLEY and A. P. DAWSON: Thapsigargin, a tumor promoter, discharges intracellular  $Ca^{2+}$  by specific inhibition of

the endoplasmic reticulum Ca<sup>2+</sup>-ATPase. Proc. Natl. Acad. Sci. U S A 87: 2466-2470  
(1990).

WOLOSIN, J. M.: Gap junctions in rabbit corneal epithelium: limited permeability and  
inhibition by cAMP. Am. J. Ophthalmol. 261: 857-864 (1991).

## LEGENDS

**Fig. 1.** (a) Light micrograph of semithin section of an epithelial sheet of cornea for  $[Ca^{2+}]_i$  measurement. The sheet is composed of superficial (S), mid wing (W) and basal (B) cell layers.  $\times 580$ . (b) Illustrations of relationship between specimen profiles and fluorescent images. Peripheral zone, mid zone and central zones of fluorescent images represent superficial, mid wing and basal cell layers, respectively.

**Fig. 2.** Ultrastructure of epithelial sheets. (a) Transverse section of the specimens. Superficial (S), mid wing (W) and basal cells (B) appear normal. N: Nuclei.  $\times 2,600$ . (b) Superficial (S) and mid wing (W) cells are connected by desmosomes (D) and interdigitation (*thick arrow*). Rough-surfaced endoplasmic reticulum (ER) and tonofilaments (TF) are evident.  $\times 40,000$ .

**Fig. 3.** Light micrographs of an epithelial sheet, showing cell viability. (a) Transmission light image of the sheet. (b) Fluorescent image of same specimen labeled by EthD-1 ( $1 \mu\text{M}$ ) after the  $[Ca^{2+}]_i$  measurement. In contrast to the isolated cells (*arrowheads*), cells of the epithelial sheet do not emit fluorescence. This indicates that the transport mechanism of cell is intact in cells of the epithelial sheet..

**Figs. 4.-7.** Time courses of ATP- and ATP-analogues-induced  $[Ca^{2+}]_i$  dynamics in various areas ( $4 \mu\text{m}^2$ ). Solid or dotted lines represent  $[Ca^{2+}]_i$  at ■ or □ in transmission light micrographs, respectively.

**Fig. 4.** When ATP (10  $\mu\text{M}$ ) is added to perfused solution,  $[\text{Ca}^{2+}]_i$  increases abruptly (spike phase; *arrow*), then a  $[\text{Ca}^{2+}]_i$  increase is sustaining during ATP stimulation (plateau phase; *arrow heads*).

**Fig. 5.** Dependence of extracellular  $\text{Ca}^{2+}$  and the intracellular  $\text{Ca}^{2+}$  store in ATP-induced  $[\text{Ca}^{2+}]_i$  dynamics. (a) Under extracellular  $\text{Ca}^{2+}$ -free conditions, ATP (10  $\mu\text{M}$ ) induces the spike phase, but not the plateau phase. (b) After depleting intracellular  $\text{Ca}^{2+}$  stores using thapsigargin (1  $\mu\text{M}$ ), ATP (10  $\mu\text{M}$ ) had no effect in  $[\text{Ca}^{2+}]_i$  dynamics.

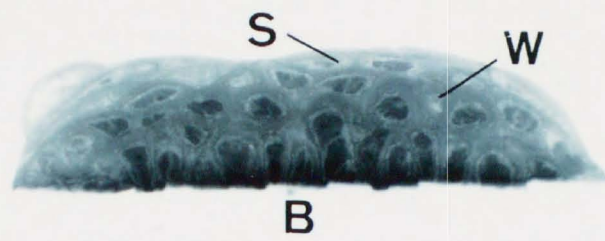
**Fig. 6.** Effect of P1 receptor agonist and P2 receptor antagonist. (a) Adenosine (10  $\mu\text{M}$ ; a P1 receptor agonist) had no effect in  $[\text{Ca}^{2+}]_i$  dynamics, in contrast to ATP (10  $\mu\text{M}$ ). (b) Suramin (100  $\mu\text{M}$ ; a P2 receptor antagonist) inhibited ATP-induced  $[\text{Ca}^{2+}]_i$  dynamics.

**Fig. 7.** Effects of ATP-analogues on  $[\text{Ca}^{2+}]_i$  dynamics. (a) UTP (10  $\mu\text{M}$ ) elicited a biphasic  $[\text{Ca}^{2+}]_i$  increase, as elicited by ATP. (b) ADP (10  $\mu\text{M}$ ) elicits a slight increase of  $[\text{Ca}^{2+}]_i$ . (c)  $\alpha,\beta$ -meATP (10  $\mu\text{M}$ ), 2-MeSATP (10  $\mu\text{M}$ ), and (d) BzATP (10  $\mu\text{M}$ ) had no effect on  $[\text{Ca}^{2+}]_i$  dynamics.

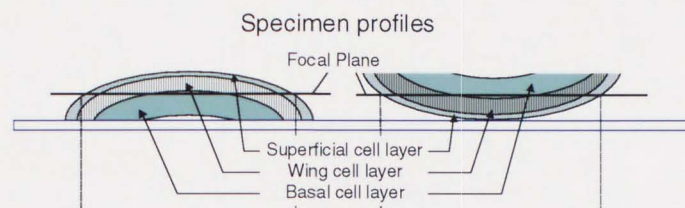
**Fig. 8.** (a) Pseudocolor images of ATP-induced  $[\text{Ca}^{2+}]_i$  dynamics in rabbit corneal epithelium. Colored points (1-4) on the transmission light image (TL image) represent colored lines (1-4) in the graphs showing time course of  $[\text{Ca}^{2+}]_i$  dynamics (b, c). (b) ATP-induced  $[\text{Ca}^{2+}]_i$  dynamics in the mid wing cell layer (red and blue areas and lines, 1 and 2). Repetitive oscillatory fluctuations are synchronized. (c) ATP-induced  $[\text{Ca}^{2+}]_i$  dynamics in the superficial (green area and line, 3) and the basal

cell layer (sky blue area and line, 4). In contrast to mid wing cells, oscillatory fluctuations are very few.

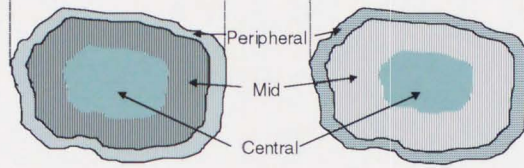
Fig.1



**a**



**b**



Fluorescent images

Fig. 2

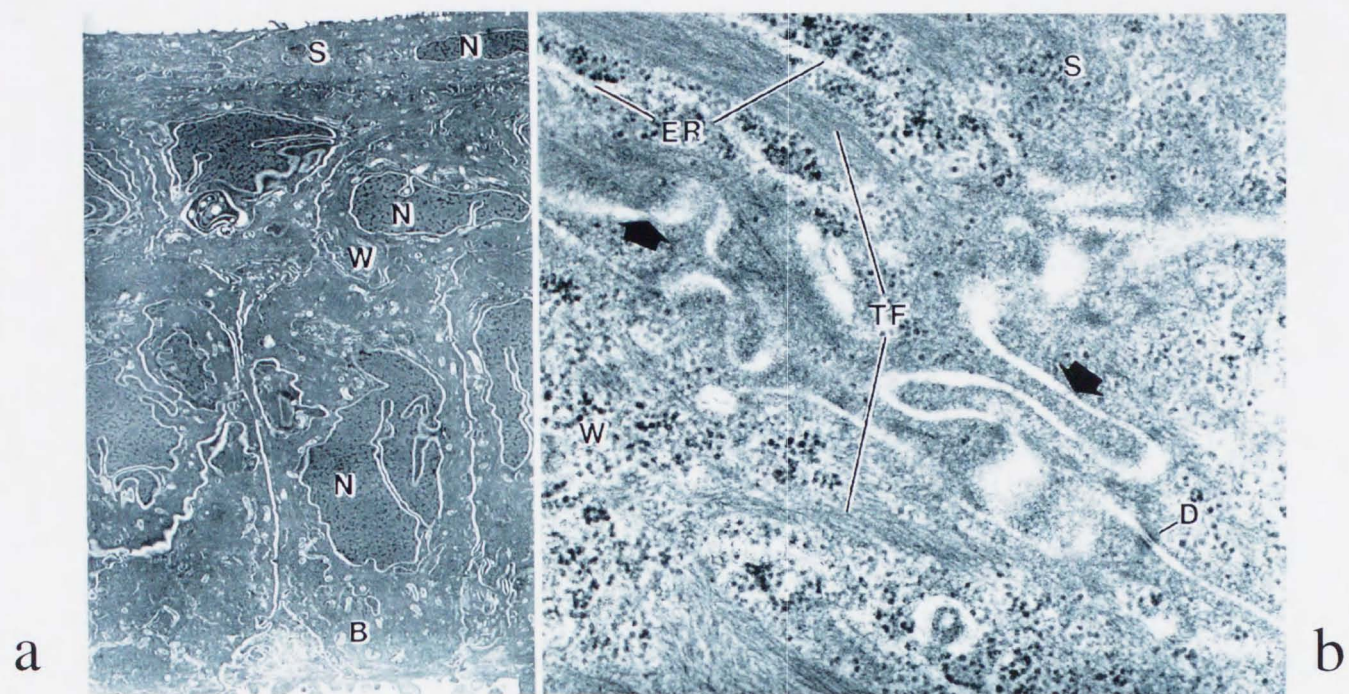


Fig. 3

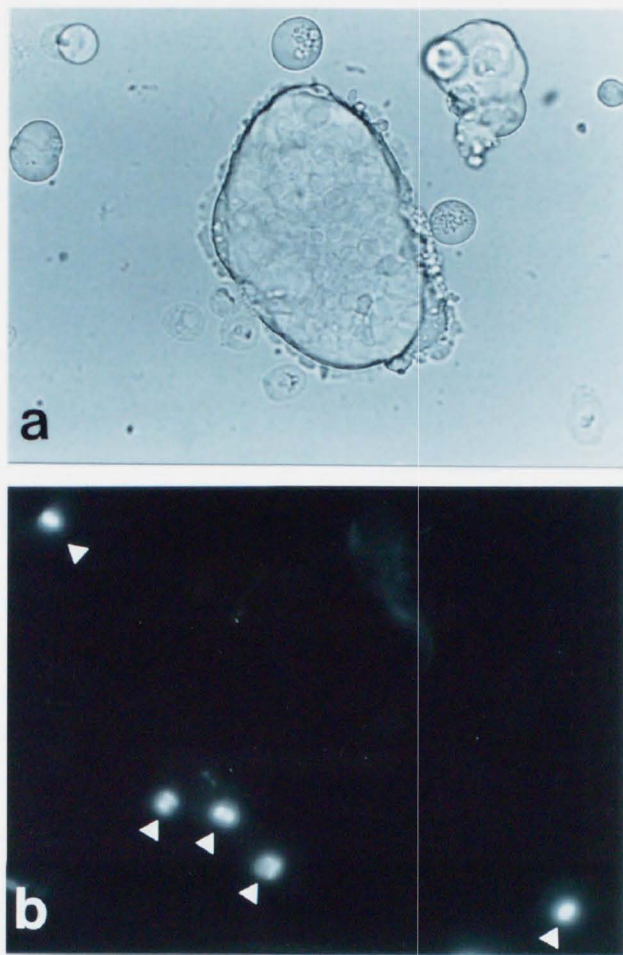


Fig. 4

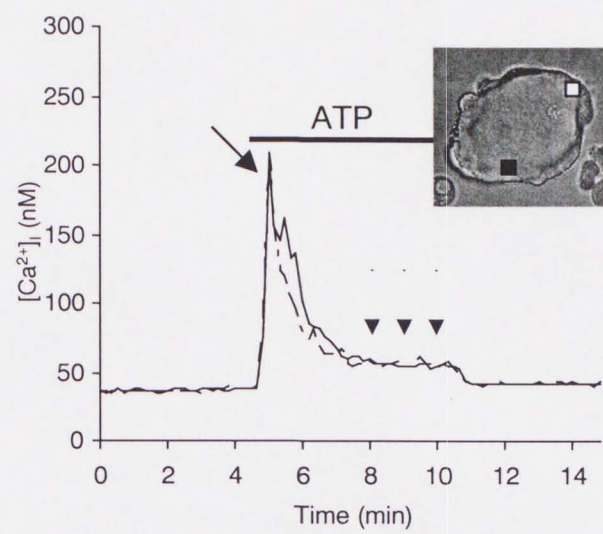


Fig. 5

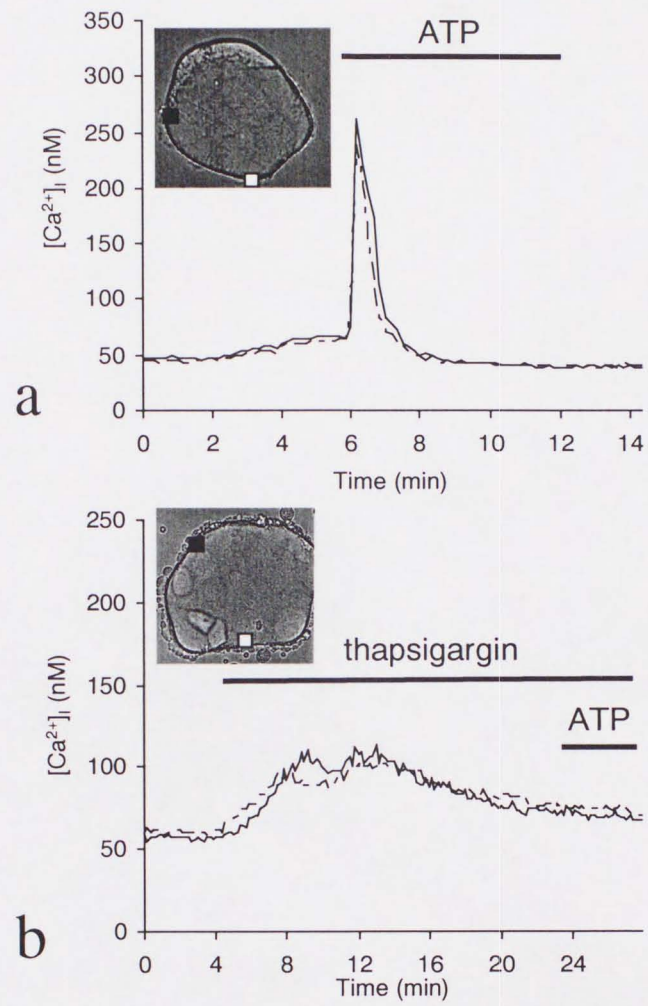


Fig. 6

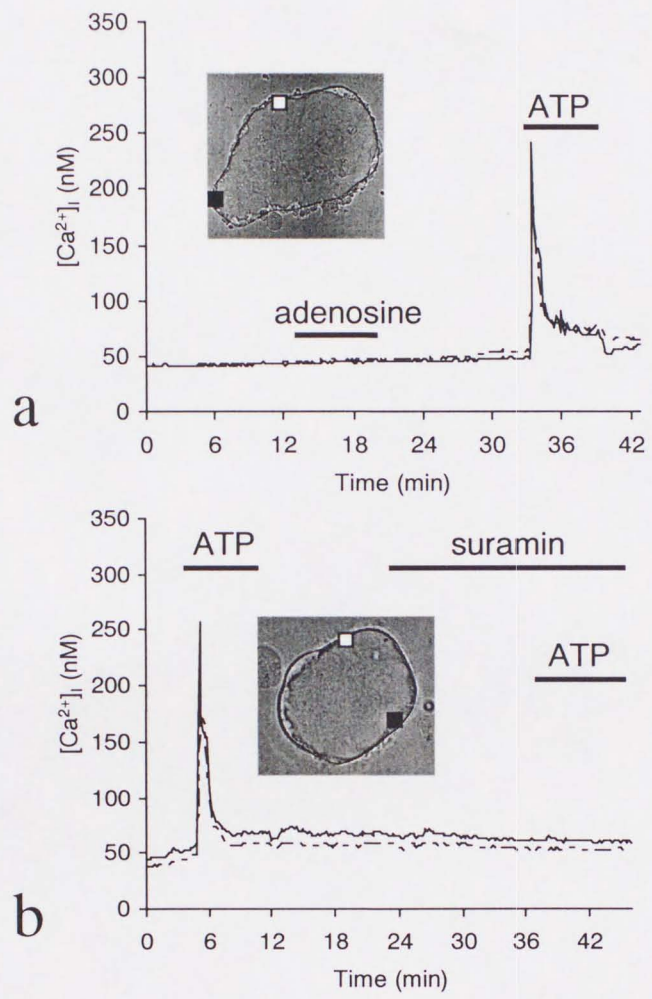


Fig. 7

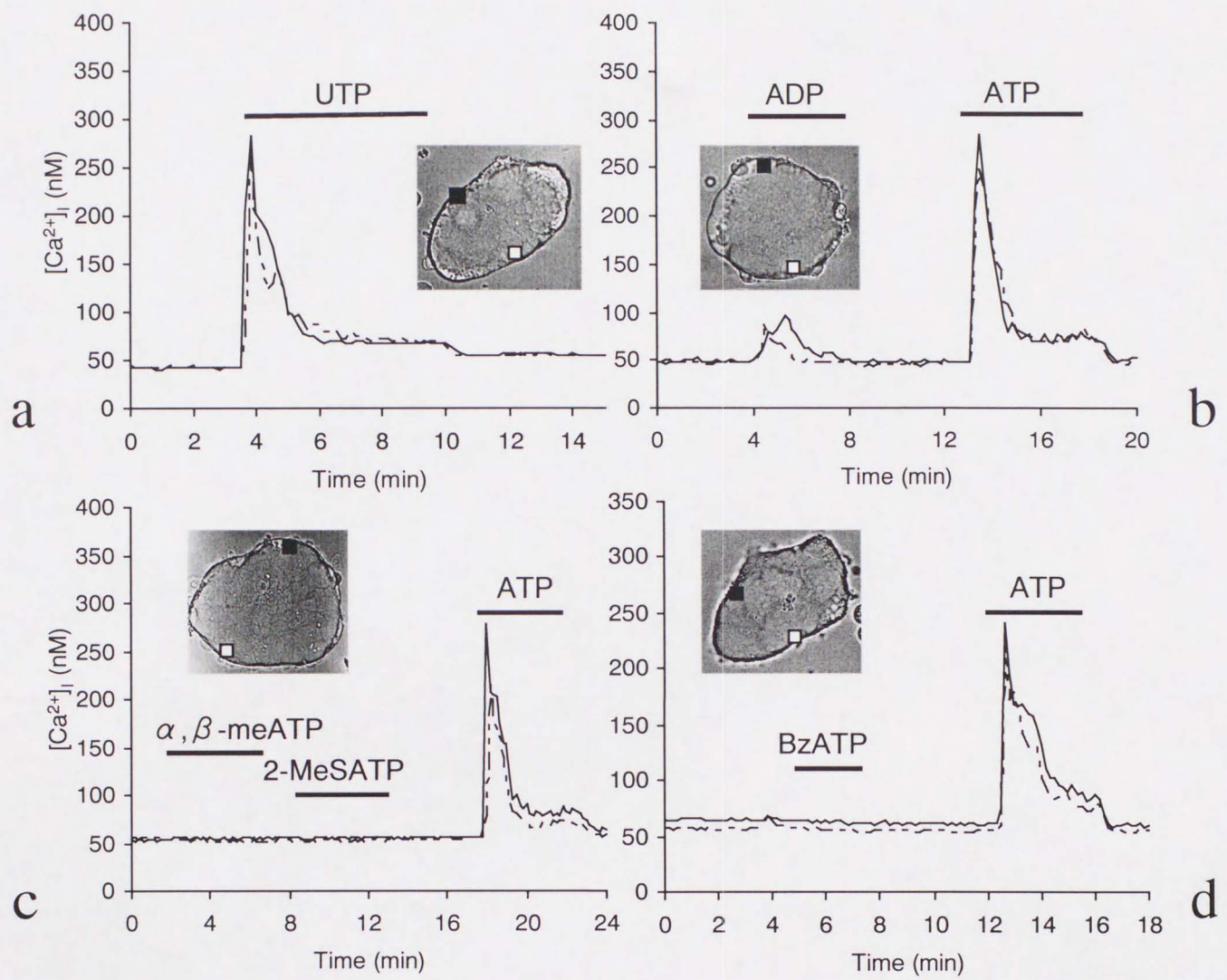
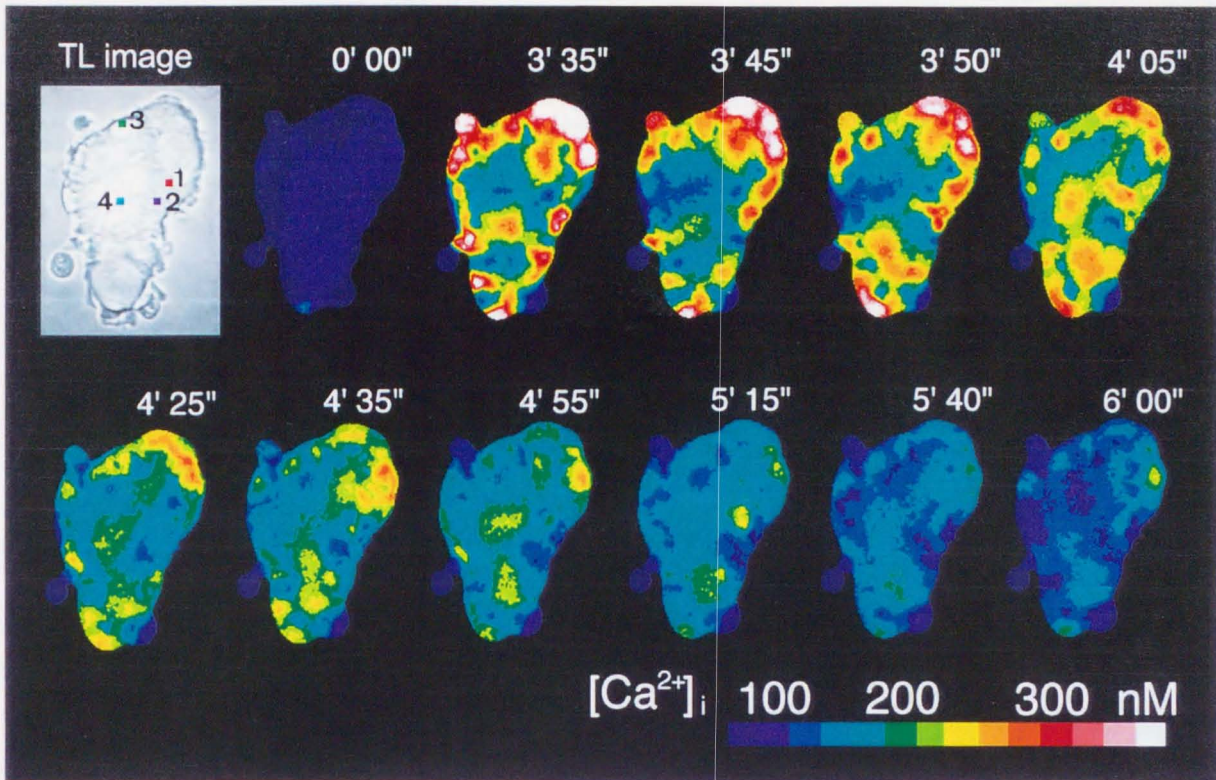
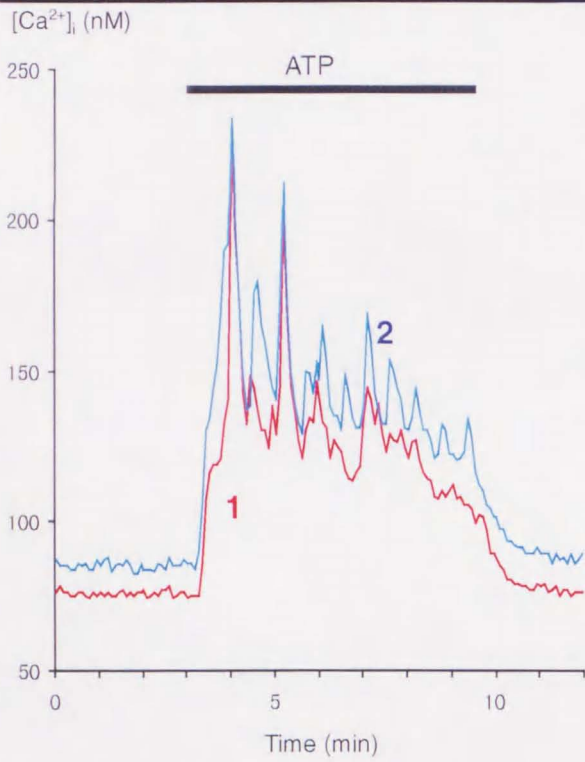


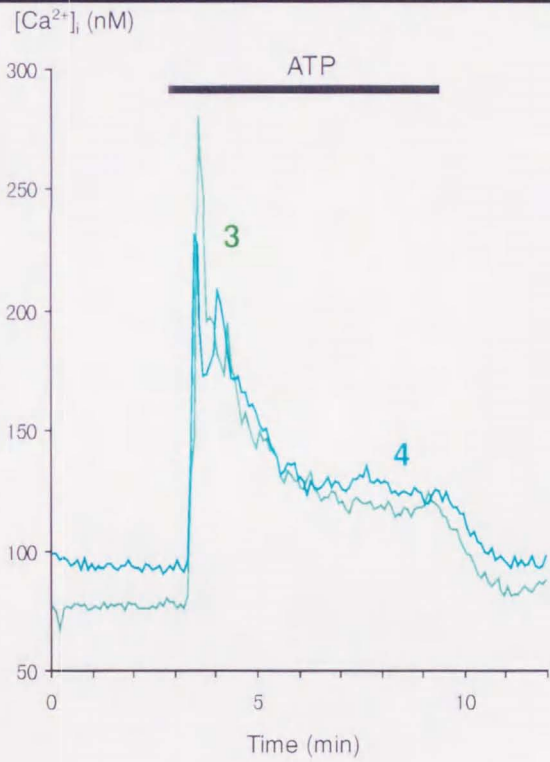
Fig 8



a



b

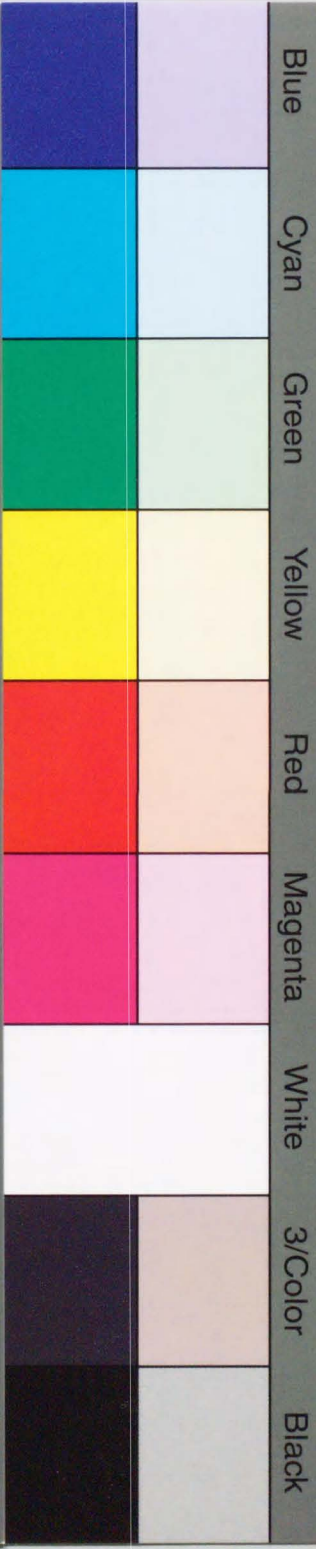


c

Inches 1 2 3 4 5 6 7 8  
cm 1 2 3 4 5 6 7 8 9 10 11 12 13 14 15 16 17 18 19

# Kodak Color Control Patches

© Kodak, 2007 TM: Kodak



Blue

Cyan

Green

Yellow

Red

Magenta

White

3/Color

Black

# Kodak Gray Scale



© Kodak, 2007 TM: Kodak

**A**

1

2

3

4

5

6

**M**

8

9

10

11

12

13

14

15

**B**

17

18

19

